New knowledge on the antiglycoxidative mechanism of chlorogenic acid

Beatriz Fernandez-Gomez[a], Monica Ullate[a], Gianluca Picariello[b], Pasquale Ferranti[b,c], Maria Dolores Mesa[d], Maria Dolores del Castillo [a]*.

[a]Department of Food Analysis and Bioactivity, Institute of Food Science Research (CIAL, CSIC-UAM), Nicolas Cabrera 9, 28049 Madrid, Spain.

[b]Istituto di Scienze dell'Alimentazione (ISA), CNR, Via Roma 52, 83100 Avellino, Italy.

[c]Department of Agriculture, University of Naples "Federico II", Parco Gussone, Portici (NA) 80055, Italy.

[d]Institute of Nutrition and Food Technology "José Mataix", University of Granada, Avenida del Conocimiento s/n Armilla, 18100 Granada, Spain.

[*]Corresponding author: Maria Dolores del Castillo, Department of Food Analysis and Bioactivity, Institute of Food Science Research (CIAL, CSIC-UAM), Nicolas Cabrera, 28049 Madrid, Spain.

Phone: +34 910017953

E-mail address: mdolores.delcastillo@csic.es

Key words: Advanced glycation end products (AGEs), chlorogenic acid, methylglyoxal, glycoxidation reaction, antiglycoxidative effect.

Abbreviations: AGEs (advanced glycation end products), MGO (methylglyoxal), GO (glyoxal), HCA (hydroxycinnamic acids), BSA (bovine serum albumin), CML (N^{ε}-(carboxymethyl)lysine), CEL (N^{ε}-(carboxyethyl)lysine), AG (aminoguanidine), 5-CQA (5-*O*-caffeoylquinic acid), 3-CQA (3-*O*-caffeoylquinic acid), CGA (3-*O*-caffeoylquinic acid)

Abstract

The mechanism of action of chlorogenic acid (CGA) on the formation of advanced glycation end-products (AGEs) (glycoxidation reaction) was studied. Model systems composed of bovine serum albumin (BSA) (1 mg mL^{-1}) and methylglyoxal (5 mM) under mimicked physiological conditions (pH 7.4, 37 ºC) were used to evaluate the antiglycoxidative effect of CGA (10 mM). The stability of CGA under reaction conditions was assayed by HPLC and MALDI-TOF MS. The glycoxidation reaction was estimated by analysis of free amino groups by OPA assay, spectral analysis of fluorescent AGEs and total AGEs by ELISA, and colour formation by absorbance at 420 nm. Structural changes in protein were evaluated by analysis of phenol-bound to protein backbone using the Folin reaction, UV-Vis spectral analysis and MALDI-TOF-MS, while changes in protein function were measured by determining antioxidant capacity using the ABTS radical cation decolourisation assay. CGA was isomerised and oxidised under our experimental conditions. Evidence of covalent binding between BSA and multiple CGA and/or its derivatives molecules (isomers and oxidation products) was found. CGA inhibited ($p < 0.05$) the formation of fluorescents and total AGEs at 72 h of reaction by 91.2 and 69.7%, respectively. The binding of phenols to BSA significantly increased ($p < 0.001$) its antioxidant capacity. A correlation was found between free amino group content, phenol-bound to protein and antioxidant capacity. Results indicate that CGA simultaneously inhibits the formation of potentially harmful compounds (AGEs) and promotes the generation of neoantioxidant structures.

1. Introduction

Protein glycation includes an initial formation of Shiff's base, followed by intermolecular rearrangement and conversion into Amadori products. They undergo further processing to form a heterogeneous group of protein-bound moieties, such as cross-linking fluorescent (*e.g.*, pentosidine) and non-fluorescent adducts (*e.g.*, N^{ε}-(carboxymethyl)lysine) (CML), N^{ε}-(carboxyethyl)lysine (CEL)) called advanced glycation end products (AGEs).[1] Pathways of AGE formation involve glucose autoxidation through the generation of α-oxoaldehydes, such as methylglyoxal (MGO), 3-deoxyglucosone and glyoxal. MGO is a major precursor of AGEs, especially CEL, which is capable of binding and modifying a number of proteins (glycoxidation reaction), including bovine serum albumin (BSA), RNase A, collagen, lysozyme and lens crystallins.[2,3] Protein glycation is known to be involved in the pathogenesis of several age-related disorders like diabetes, atherosclerosis, end-stage renal and neurodegenerative diseases.[4]

Inhibitors of AGEs formation might follow several mechanisms, such as aldose reductase, antioxidant activity, reactive dicarbonyl trapping, sugar autoxidation inhibition and amino group binding.[5] The inhibition of AGE formation by synthetic aminoguanidine (AG) has been widely documented. However, as AG treatment in type 1 diabetics has caused serious complications, the search for natural AGE inhibitors is currently a challenge. [6]

Coffee and yerba mate are considered natural sources of abundant phenolic compounds that can inhibit the formation of AGEs.[7,8] The most representative phenolic acids in these foods are chlorogenic acids (CGA), which commonly occur as 5-*O*-caffeoylquinic acid (5-CQA) or 3-*O*-caffeoylquinic acid (3-CQA).[9,10] The antiglycation activity of CGA has been associated to its antioxidant and chelating characters, as well as to its ability to trap reactive dicarbonyl compounds.[8,11] This study aimed to obtain a better understanding of the antiglycoxidative mechanism of action of CGA which is partly unknown. *In vitro* studies mimicking physiological conditions were performed to achieve this goal.

2. Materials and methods

2.1 Materials

All chemicals and solvents were of analytical grade. Bovine serum albumin (BSA), phosphate buffered saline (PBS), 3-*O*-caffeoylquinic acid (CGA), sodium azide, *ortho*-phthaldialdehyde (OPA), N^{α}-acetyl-L-lysine, Folin-Ciocalteau, 3.3′, 5.5′-Tetramethylbenzidine (TMB) were from Sigma–Aldrich (St. Louis, USA). Other chemicals and their suppliers were as follows: *β*-mercaptoethanol (Merck, Hohenbrunn, Germany), methylglyoxal solution (MGO) and 2.2'-azino-bis (3-ethylbenzothiazoline-6-sulphonic acid) diammonium salt (ABTS) (Fluka, Buchs, Switzerland) and Bradford reagent for protein assay (Bio-Rad, München, Germany). The Amicon® Ultra- 0.5 ml centrifugal filter unit fitted with an Ultracel®-30K regenerated cellulose membrane (30 kDa cut-off) was from Merck Millipore Ltd. (Tullagreen, Cork, Ireland). Microtest 96-well plates made from high-quality polystyrene were purchased from Sarstedt AG & Co. (Nümbrecht, Germany). The Costar® high binding 96-well EIA/RIA plate was from Corning Incorporated (Corning, NY, USA). The Milli-Q water used in this study was obtained using a purification system (Millipore, Molsheim, France).

2.2 Formation of CGA derivatives in control samples

2.2.1 HPLC analysis

Standard CGA before and after incubation at 37 ºC for 24 h were compared to assess the chemical stability of the compound under experimental conditions by reversed phase (RP) HPLC. A modular chromatographer HP 1100 (Agilent Technologies, Paolo Alto, CA, USA) equipped with a multi-waves UV-Vis detector was used to analyse samples. The stationary phase was a 250 x 2.1 mm i.d. C18 RP column, particle diameter 4 μm (Jupiter Phenomenex, Torrance, CA, USA). Column temperature was maintained at 37 °C during the HPLC analyses. Separations were carried out at a constant flow rate of 0.2 mL min^{-1} applying a 5-60% linear gradient of solvent B (acetonitrile/ 0.1% trifluoroacetic acid, TFA) over 60 min, after 5 min of isocratic elution at 5% solvent B. Solvent A was 0.1% TFA in HPLC-grade water. For each run, 2.5 μg standard or incubated CGA were diluted 10-fold with 0.1% TFA and injected using a Rheodyne® valve. The

HPLC separations were monitored at 280, 320 and 360 nm, while UV-Vis spectra (200-600 nm) were recorded using a diode array detector.

2.2.2 MALDI-TOF-MS analysis

Mass spectra of CGA freshly prepared and incubated at 37 ºC for 24 h were acquired on a Voyager DE-Pro spectrometer (PerSeptive BioSystems, Framingham, Massachusetts) equipped with a N_2 laser (λ= 337 nm) operating in both positive and negative reflector ion modes. The matrix was 2.5- hydroxybenzoic acid (DHB) 10 mg mL^{-1} in 50% acetonitrile. In the positive ion mode, the matrix solution also contained 0.1% TFA. Spectra were acquired using Delay Extraction technology at an accelerating voltage of 20 kV, exploring the *m/z* 150−1200 range. Matrix ion signals were excluded by separately acquiring positive and negative spectra of DHB. The mass range was externally calibrated with a mixture of standard polyphenols (Sigma, Milan, Italy). Spectra were elaborated with Data Explorer 4.0.

2.3 *In vitro* glycoxidation of proteins

Model systems were composed of BSA at a final concentration of 1 mg mL^{-1} in 0.01 M PBS buffer (pH 7.4) added with sodium azide (0.05%) and MGO (5 mM). Glycoxidation model systems were prepared in the presence or absence of the inhibitor (CGA 10 mM). Prior to initiation of the glycoxidation reaction by addition of MGO, the pH values of all solutions were measured at 25 °C using an electrode pH-meter (Metler Toledo, Spain) to ensure optimal and equal conditions of reaction in all samples (pH=7.4). The model systems were incubated at 37 °C for 192 h, and samples were taken after 24, 72, 96 and 192 h. The glycoxidation reaction was stopped by cooling in an ice bath. All samples were prepared in triplicate. A control solution of BSA was also included. The progress of the glycoxidation reaction was determined by analysing free amino groups, AGEs and brown compounds.

2.3.1 Free amino groups

Free protein amino groups (both N-terminal and epsilon -NH_2 of lysine) were determined by the OPA assay, following Go *et al*.[12] OPA reagent was freshly prepared by dissolving 10 mg of OPA in 250 µL of 95% (v/v) ethanol and adding 9.8 mL of 0.01 M PBS pH 7.4 and 20 µL of *β*-mercaptoethanol. The total volume of reaction was 250 µL. The reaction was carried out in transparent polystyrene 96-well microtest plate (No. 82.1581). Fluorescence was read after the addition of OPA reagent on a microplate fluorescence reader Biotek Synergy™ HT (Biotek Instruments, Highland Park, Winooski, USA) with excitation at 360 ± 40 nm and emission at 460 ± 40 nm. Fluorescence was read every 53 s for 15 min. Calibration curves were constructed using standard solutions of N^{α}-acetyl-L-lysine (0.025-1 mM). All measurements were performed in triplicate, and data were expressed as µg N^{α}-acetyl-L-lysine equivalent per mg of protein.

2.3.2 AGEs

AGE formation was monitored by fluorescence spectrophotometry using a Biotek microplate spectrophotometer at 360 ± 40 nm and 460 ± 40 nm as excitation and emission wavelengths, respectively. No dilution was required for the glycoxidation model or the control systems. All measurements were performed in triplicate.

The formation of total AGEs-BSA was measured by an indirect ELISA assay in samples incubated for 72 h. A high affinity protein 96-well microplate was coated overnight (4° C) with 100 µL of protein samples in 0.01 M phosphate buffer (pH 7.4) (5 µg mL^{-1}). Unbound proteins were washed out with buffer PBS-T (PBS 0.01 M; Tween 0.05%), the wells were blocked with gelatin 0.5% for 1 h at room temperature, then washed out with PBS-T, and the primary antibody (dilution 1:1000) was added for 1 h. A polyclonal rabbit IG antibody which rose against AGEs (AGE 102-0.2, Biologo, Kroshagen, Germany) was used as the primary antibody. After 1 h incubation and five washing steps, the secondary horse radish peroxidise-conjugated mouse anti-rabbit IgG antibody (ABIN376294, antibodies-online Inc.,Suite, Atlanta) diluted 1:4000 in washing buffer PBS-T was added, incubated for 1 h and washed again. Colour was developed with TMB (100 µL) and absorbance was read at 650 nm. Values were estimated by comparison

161 with a standard curve of glycated BSA (Methylglyoxal-AGE-BSA, CY-R2062, CircuLex™,
162 CycLex Co., Ltd, Nagano, Japan). All measurements were performed in triplicate, and results
163 were expressed as µg of AGEs-BSA per mg of protein.

164 2.3.3 Brown pigments

165 Formation of brown pigments in the samples was estimated by measuring absorbance at 420 nm
166 of the samples at 24, 72, 96 and 192 h, using microplate reader BioTek PowerWave™ XS.
167 Samples were analysed in triplicate.

168 2.4 Structural changes of proteins

169 Prior to analysis, the protein fraction of samples incubated at 37 ºC for 72 h was isolated by
170 ultrafiltration. Samples (0.4 mL) were placed in the sample reservoir of an Amicon® Ultra- 0.5 mL
171 centrifugal filter unit fitted with an Ultracel®-30K regenerated cellulose membrane (30 kDa cut-
172 off) (Millipore Ltd., Ireland) and centrifuged at 14000 g for 40 min at room temperature. The
173 concentrated samples were recovered and diluted in PBS (0.4 mL). Protein concentration was
174 determined by the Bradford micromethod. The isolated protein fraction was used for structural and
175 functional characterisation.

176 2.4.1 UV-Vis spectra

177 A Biotek microplate UV-Vis spectrophotometer equipped with UV KC junior software (Biotek)
178 was used. The spectrum of fractionated samples was measured at 200-790 nm using a quartz 96-
179 well microplate.

180 2.4.2 Total phenolic compounds

181 Total phenolic content (TPC) of the isolated fraction incubated for 72 h was determined using the
182 Folin-Ciocalteu method as described by Singleton *et al.*[13] adapted to a microplate reader. The
183 reduction reaction was carried out in 210 µL total volume in 96-well microplates (No. 82.1581).

A 10 µL of sample (appropriately diluted when necessary) was added to 150 µl volume of Folin-Ciocalteu reagent (diluted 1:14, v/v) in Milli-Q water. After exactly 3 minutes, 4 mL of 75 g L^{-1} sodium carbonate solution and 6 mL of water were mixed, and 50 µL of this mixture was added to each well. Absorbance at 750 nm was recorded using a microplate reader BioTek PowerWave™ XS. Calibration curves were constructed using standard solutions of CGA (0.1-1 mg L^{-1}), and results were expressed as µg CGA mL^{-1}.

2.4.3 MALDI-TOF-MS analysis

MALDI-TOF mass spectra of samples incubated for 72 h were acquired in the linear positive ion mode using Voyager DE-Pro spectrometer (PerSeptive BioSystems, Framingham, Massachusetts). The accelerating voltage was 25 kV. Sinapinic acid (10 mg L^{-1} in 50% acetonitrile/TFA 0.1%) was used as the matrix. Spectra were externally calibrated using a commercial protein mixture provided by the instrument manufacturer (PerSeptive Biosystems, Framingham, Massachusetts).

2.5 Functionality changes in proteins

The antioxidant capacity of samples incubated for 72 h was estimated by the $ABTS^{\bullet+}$ decolourisation assay as described by Oki *et al.*[14] 2.2'-azino-bis (3-ethylbenzothiazoline-6-sulfonic) acid radical cations ($ABTS^{\bullet+}$) were produced by reacting 7 mM ABTS stock solution with 2.45 mM potassium persulfate and allowing the mixture to stand in the dark at room temperature for 12-16 h before use. The $ABTS^{\bullet+}$ solution (stable for 2 d) was diluted in 5 mM PBS pH 7.4 (1:16 v/v) to an absorbance of 0.70 ± 0.02 at 734 nm. Each sample was dissolved in phosphate buffer (5 mM, pH 7.4) at 0.1 mg L^{-1}. Thirty µL of test sample and 200 µL of diluted ABTS•+ solution were mixed. Absorbance of the samples at 734 nm was measured at 10 min of reaction using BioTek Power Wave™ XS microplate reader. CGA at concentrations of 0.015-0.2 mM was used for calibration.

2.6 Statistical analysis

Data were expressed as mean ± standard deviation (SD). Analysis of Variance (more than 2 groups), one-way and two-way ANOVA followed by Bonferroni test, were applied to determine differences between means. Differences were considered to be significant at $p < 0.05$. Relationships between the analysed parameters were evaluated by computing Pearson linear correlation coefficients setting the level of significance at $p < 0.001$.

3. Results

3.1 Formation of CGA derivatives

Fig. 1a compares the HPLC chromatograms of standard CGA before (lower panel) and after incubation at pH 7.4, 37 ºC for 24 h (upper panel). Peaks were assigned based on retention times and UV-Vis spectra. Under our experimental conditions, CGA was converted into two isomers, namely neochlorogenic acid (trans-5-*O*-Caffeoylquinic acid) and cryptochlorogenic acid (4-*O*-Caffeoylquinic acid).

The MALDI-TOF-MS (Fig. 1b) demonstrated the co-occurrence of the hydroquinone and quinone forms ($[M + H]^+$ *m/z* 353 and *m/z* 355, and $[M + Na]^+$ *m/z* 375 and *m/z* 377, respectively) along with the dimeric adducts ($[2M + Na]^+$ *m/z* 729 and *m/z* 731), as assigned in the Table 1. No CGA homopolymers were detected by either HPLC or MALDI-TOF-MS.

3.2 Progress of the glycoxidation reaction

The availability of free amino groups was obtained by OPA assay (Fig. 2). Incubation of BSA alone at 37 ˚C for 192 h did not significantly affect ($p > 0.001$) the availability of free amino groups, indicating the absence of inter-protein cross-linking events. Incubation in the presence of MGO produced a significant decrease ($p < 0.001$) in BSA free amino groups during the incubation period, suggesting that the glycoxidation reaction occurred. Interestingly, the addition of CGA to the glycoxidation mixture (BSA+MGO) also caused a significant decrease ($p < 0.001$) in available free amino groups throughout the whole incubation period. Available free amino groups also decreased when BSA was incubated with CGA alone compared to the protein control and did not

significantly differ ($p > 0.001$) from those of the inhibition model composed of BSA, MGO and CGA.

Fig. 3 illustrates the formation of fluorescent AGEs during 192 h of glycoxidation reaction. As expected, the protein control (BSA alone) showed very low fluorescence intensity throughout the experiment, due to intrinsic fluorescence caused by the presence of fluorescent amino acids in the protein backbone. The reaction of BSA and MGO produced a significant formation ($p < 0.05$) of fluorescent AGEs in a time dependent manner. The presence of CGA efficiently inhibited ($p < 0.05$) fluorescent AGE formation in the glycoxidation model system, while the reaction of BSA and CGA caused a minor formation of fluorescent compounds. Further and more precise information regarding the generation of total AGEs, both fluorescent and non-fluorescence adducts, under our experimental conditions was obtained by indirect ELISA (Table 2). The results are consistent with those obtained by fluorescence monitoring. BSA data are considered basal values for all model systems. AGE generation was significantly ($p < 0.05$) inhibited by the presence of CGA in the glycoxidation system.

Fig. 4 shows the generation of brown compounds. Absorbance values at 420 nm of mixtures composed of BSA alone and BSA+MGO were very low and not significantly different ($p > 0.05$) in any case. The presence of CGA in the model systems induced significant brown compound formation in a time dependent manner. High and similar levels of browning ($p > 0.05$) were found in model systems composed of CGA alone and BSA+CGA. The extent of brown compound formation in samples composed of BSA, MGO and CGA was significantly lower ($p < 0.05$) than in the other samples containing CGA.

3.3 Structural changes of protein

Since significant AGE formation was observed after 72 h of glycoxidation reaction (Fig. 3 and Table 2), those samples were selected for further characterisation. As shown in Fig. 5a, fresh and incubated (37 ˚C for 72 h) BSA solutions exhibited identical UV-Vis spectra, suggesting that no

structural modifications of proteins occurred following heating. Furthermore, the glycoxidation reaction BSA+MGO did not alter the UV-Vis spectrum compared to fresh BSA. In contrast, the protein fraction isolated from the glycoxidation mixture with CGA showed a very different spectrum than that found for the control (BSA) and was very similar to the spectrum of BSA incubated with CGA.

Total phenolic content of the samples incubated at pH 7.4, 37 ºC for 72 h is shown in Fig. 5b. As expected, significant levels ($p < 0.05$) of phenolic compounds were detected in the protein fractions isolated from the CGA model systems, namely BSA + CGA and BSA + MGO + CGA.

MALDI-TOF-MS analysis was performed to confirm the formation of covalent bindings of CGA to the protein backbone at 72 h (Fig. 6). In the spectra corresponding to BSA incubated with MGO, the characteristic peak of BSA was clearly visible with variable mass increases (Fig. 6b). Greater mass shifts were observed when BSA was incubated with CGA either in the absence (Fig. 6c) or presence of MGO (Fig. 6d). The mass data suggested that, BSA binds several molecules of CGA and its derivatives in addition to the MGO in these samples, forming a heterogeneous mixture of protein conjugates as reflected by the broadening of BSA peaks (Fig. 6c and 6d).

3.4 Changes of protein function

The antioxidant capacity of the isolated protein fractions obtained from samples incubated at 37 ºC for 72 h is shown in Fig. 7. The reaction with MGO did not modify the antioxidant capacity of BSA. The addition of CGA to reaction mixtures caused the formation of compounds (MW > 30 kDa) which had antioxidant capacity values of 303.07 and 309.89 μg eq-CGA mL^{-1} for model system composed of BSA+MGO+CGA and BSA+CGA, respectively.

3.5. Correlation between parameters

A significant negative correlation ($r=-0.754$, $p < 0.001$) between data corresponding to free amino groups and antioxidant capacity was observed for samples incubated at 37 ºC for 72h. A

significant negative correlation ($r=-0.689$, $p < 0.001$) was also found between free amino groups and total phenolic content.

4. Discussion

In this work we observed that structural changes in CGA produced *in vitro* under mimicked physiological conditions may contribute to the antiglycoxidative properties of this compound. Isomerisation of CGA (3-*O*-caffeoylquinic acid) was induced at pH 7.4 and 37 ºC. The formation of neochlorogenic (trans-5-*O*-caffeoylquinic acid) and cryptocholorogenic (4-*O*-caffeoylquinic acid) acid from CGA under similar reaction conditions has previously been reported.[15,17] CGA derivatives such as oxidation products and isomers might be able to act as substrate or/and precursors of the Maillard and polymerisation reactions. [18] The formation of mono-quinones and dimer quinones was also observed in CGA incubated at pH 7.4 and 37 ºC for 24 h. This is in agreement with the non-enzymatic oxidation of CGA described by Rawel et al.[19]

Brown compounds may be formed by the Maillard reaction, oxidation of phenols and phenol polymerisation.[18] Our data suggest that the Maillard and phenol oxidation reactions are the main pathways leading to the formation of brown compounds under our experimental conditions. Both CGA and its derivatives are able to react with BSA via the Maillard reaction. However, further studies are needed to determine the chemical nature of new-formed coloured compounds.

The observed decrease in the formation of AGEs in the presence of CGA demonstrates the antiglycative activity of this compound. On the other hand, our results suggest conjugation of CGA or its derivatives to free amino groups. A significant negative correlation between content of free amino groups and phenolic compounds was found. These results are in agreement with Rawel et al.[20] who reported a decrease in lysine residues due to the reaction of BSA and CGA at room temperature for 24 h. CGA isomers and quinones can interact with proteins forming non-covalent and covalent bonds through the Maillard Reaction[18]. Phenolics bind highly nucleophilic thiol, amine groups and hydrophobic aromatic groups of proteins.[21] Three potential types of non-covalent interactions between hydroxycinnamic acids and proteins have been proposed: hydrogen,

311 hydrophobic, and ionic binding. [22] Prigent et al.[21] found that oxidised CGA induced covalent
312 modification of α-lactalbumin and lysozyme.

313 Soft ionization MS techniques such as MALDI are useful to evaluate the hydroxycinnamates
314 (HCA) covalently bound to proteins.[20] MALDI-TOF-MS data suggest the formation of
315 neoformed protein-phenol conjugates, inducing MS increments of 1.7 and 1.3 kDa in samples
316 corresponding to BSA+CGA and BSA+CGA+MGO, respectively. The increase of molecular
317 mass is indicative of covalent binding between CGA and/or its derivatives to the protein structure.
318 Data on MALDI-TOF-MS support the data obtained on free amino groups, phenolic compounds
319 and UV-Vis spectra.

320 The formation of complexes by covalent binding of other reactive phenols such as quercetin to
321 BSA exhibiting antioxidant potential have been previously reported.[23,24] Quercetin and CGA share
322 a high binding affinity for BSA. The ability of these two compounds to form covalent complexes
323 polyphenol-BSA under physiological conditions has been demonstrated.[25,26] Our results show that
324 CGA causes the neoformation of molecules with antioxidant capacity.

325 Gugliucci et al.[8] previously associated the inhibitory capacity against formation of fluorescent
326 AGEs of *Ilex paraguariensis* extracts to the presence of CGA. The inhibitory capacity of CGA
327 was linked to its antioxidant character, chelating properties to transition metals ions, quenching of
328 carbonyl radical species and AGE crosslinking.[27-29] Other authors have also shown the ability of
329 CGA to inhibit *in vitro* BSA glycation induced by fructose and glucose and the formation of AGE
330 crosslinking from collagen.[11] We have recently reported that MGO is effectively trapped by CGA
331 with an IC_{50} of 0.14 mg mL^{-1}.[30] In addition to this mechanism, we propose for the first time a
332 relationship between the high binding capacity of CGA to BSA and its antiglycoxidative
333 mechanism of action. The covalent interactions suggest MGO and GCA are competing for reactive
334 protein sites (free amine group). This effect prevents MGO from binding to BSA resulting in an
335 effective decrease in AGE formation.

Coffee is the major source of CGA on the worldwide diet. CGA from coffee has shown a high bioavailability in humans.[31] Previous studies suggest that consumption of coffee acutely increases the concentrations of phenolic compounds in LDL cholesterol particles and platelets, increases *ex vivo* resistance to LDL oxidation, and reduces platelet aggregation in healthy volunteers. [32,33] These results support formation of antioxidant polyphenol-protein complexes *in vivo* and *ex vivo* with health promoting properties. Formation of polyphenol-protein complexes *in vivo* is feasible and it may be associated to a reduction of risk of diabetes complications such as cardiovascular disease.

In summary, the covalent conjugation of CGA and its derivatives (isomers and quinones) to side-chains of protein lysine residues reduces the formation of potentially harmful compounds, also called AGEs, and promotes the generation of antioxidant structures, which may be beneficial for human health.

Acknowledgements

This study was funded by the projects: AGL2010-17779 and IT2009-0087. B Fernandez is grateful for a FPI-predoc grant from the Ministry of Economy and Competitiveness (Spain).

References

1. R. B. Nawale, V.K. Mourya and S. B. Bhise, Non-enzymatic glycation of proteins: a cause for complications in diabetes, *Indian J. Biochem. Bio.*, 2006, **43**, 337-344.
2. Z. Kender, P. Torzsa, K. V. Grolmusz, A. Patócs, A. Lichthammer, M. Veresné Bálint, K. Rácz and P. Reismann, The role of methylglyoxal metabolism in type-2 diabetes and its complications, *Orv. Hetil*, 2012, **153**, 574-585.
3. K. V. Tarwadi and V. V. Agte, Effect of micronutrients on methylglyoxal-mediated in vitro glycation of albumin, *Biol. Trace Elem. Res.*, 2011, **143**, 717-725.
4. N. Ahmed, Advanced glycation endproducts-role in pathology of diabetic complications**,** *Diabetes Res. Clin. Pr.*, 2005, **67**, 3-21.
5. I. Bousová, J. Martin, L. Jahodár, J. Dusek, V. Palicka and J. Drsata, Evaluation of in vitro effects of natural substances of plant origin using a model protein glycoxidation. *J Pharmaceut. Biomed.*, 2005, **37**, 957-962.
6. P. J. Thornalley, Use of aminoguanidine (Pimagedine) to prevent the formation of advanced glycation endproducts, *Arch. Biochem. Biophys.*, 2003, **419**, 31-40.
7. E. Verzelloni, D. Tagliazucchi, D. Del Rio, L. Calani and A. Conte, Antiglycative and antioxidative properties of coffee fractions, *Food Chem.*, 2011, **124**, 1430-1435.
8. A. Gugliucci, D. H. Markowicz Bastos, J. Schulze and M. Ferreira Souza, Caffeic and chlorogenic acids in *Ilex paraguariensis* extracts are the main inhibitors of AGE generation by methylglyoxal in model proteins, *Fitoterapia*, 2009, **80**, 339-344.
9. M. N. Clifford, Chlorogenic acids and other cinnamates—nature, occurrence, dietary burden, absorption and metabolism, *J. Agric. Food Chem.*, 2000, **80**, 1033-1043.
10. S. Meng, J. Cao, Q. Feng, J. Peng and Y. Hu, Roles of chlorogenic acid on regulating glucose and lipids metabolism: a review, *Evid. Based Complement. Alternat. Med.*, 2013, DOI: 10.1155/2013/801457.

11. J. Kim, I. H. Jeong, C. S. Kim, Y. M. Lee, J. M. Kim and J. S. Kim, Chlorogenic acid inhibits the formation of advanced glycation end products and associated protein cross-linking, *Arch. Pharmacal. Res.*, 2011, **34**, 495-500.
12. K. Go, R. Garcia and F. J. Villarreal, Fluorescent method for detection of cleaved collagens using *O*-phthaldialdehyde (OPA), *J. Biochem. Biophys. Methods*, 2008, **70**, 878-882.
13. V. L. Singleton, R. Orthofer and R. M. Lamuela-Reventós, Analysis of total phenols and other oxidation substrates and antioxidants by means of Folin-Ciocalteu reagent, *Methods Enzymol.*, 1999, **299**, 152-178.
14. T. Oki, M. Masuda, S. Furuta, Y. Nishiba, N. Terahara and I. Suda, Involvement of anthocyanins and other phenolic compounds in radical-scavenging activity of purple-fleshed sweet potato cultivars, *J. Food Sci*., 2002, **67**, 1752-1756.
15. S. Li and C.T. Ho, Stability and transformation of bioactive polyphenolic components of herbs in physiological pH. In Herbs: Challenges in Chemistry and Biology, ed. American Chemical Society, 2006, ch. 18, pp. 240-253.
16. S. Deshpande, R. Jaiswal, M.F. Matei and N. Kuhnert. Investigation of acyl migration in mono- and dicaffeoylquinic acids under aqueous basic, aqueous acidic, and dry roasting conditions, *J. Agric. Food Chem*., 2014, **37**, 9160-9170.
17. C. Xie, K. Yu, D. Zhong, T. Yuan, F. Ye, J. A. Jarrell, A. Millar and X. Chen, Investigation of isomeric transformations of chlorogenic acid in buffers and biological matrixes by ultraperformance liquid chromatography coupled with hybrid quadrupole/ion mobility/orthogonal acceleration time-of-flight mass spectrometry. *J. Agric. Food Chem*., 2011, **59**, 11078-11087.
18. Z. Budryn and D. Rachwal-Rosiak, Interactions of hydroxycinnamic acids with proteins and their technological and nutritional implications, *Food Rev. Int*., 2013, **29**, 217-230.
19. H. M. Rawel and S. Rohn, Nature of hydroxycinnamate-protein interactions, *Phytochem. Rev.*, 2010, **9**, 93-109.
20. H. M. Rawel, S. Rohn, H. P. Kruse and J. Kroll, Structural changes induced in bovine serum albumin by covalent attachment of chlorogenic acid, *Food Chem*., 2002, **78**, 443-455.

21. S. V. Prigent, A. G. Voragen, A. J. Visser, G. A. van Koningsveld and H. Gruppen, Covalent interactions between proteins and oxidation products of caffeoylquinic acid (chlorogenic acid), *J. Sci. Food Agric*., 2007, **87**, 2502-2510.
22. T. Dan , L. Hui-Jun, L. Ping , W. Xiao-Dong and Q. Zheng-Ming, Interaction of bioactive components caffeoylquinic acid derivatives in chinese medicines with bovine serum albumin, *Chem. Pharm. Bull*., 2008, **56**, 360-365.
23. R. Sascha, H. M. Rawel and J. Kroll, Antioxidant activity of protein-bound quercetin, *J. Agric. Food Chem*., 2004, **52**, 4725-4729.
24. X. Y. Dong, H. F. Yao, F. Z. Ren and H. Jing, Characteristics and antioxidant activity of bovine serum albumin and quercetin interaction in different solvent systems, *Spectrosc. Spect. Anal*., 2014, **34**, 162-166.
25. Y. Ni, X. Zhangb and S. Kokotc, Spectrometric and voltammetric studies of the interaction between quercetin and bovine serum albumin using warfarin as site marker with the aid of chemometrics, *Food Chem*., 2006, **99**, 191-203.
26. L. Trnkova, I. Bousova, V. Kubicek and J. Drsata, Binding of naturally occurring hydroxycinnamic acids to bovine serum albumin, *Natural Science*, 2010, **6**, 563-570.
27. H. Y. Kim and K. Kim, Protein glycation inhibitory and antioxidative activities of some plant extracts in vitro, *J. Agric. Food Chem.*, 2003, **51**, 1586-1591.
28. S. Sang, X. Shao, N. Bai, C. Y. Lo, C. S. Yang and C. T. Ho, Tea polyphenols (−)epigallocatechin-3-gallate:A new trapping agent of reactive dicarbonyl species, *Chem. Res. Toxicol.*, 2007, **20**, 1862-1870.
29. C. H. Wu and G. C. Yen, Inhibitory effect of naturally occurring flavonoids on the formation of advanced glycation endproducts, *J. Agric. Food Chem.*, 2005, **53**, 3167-3173.
30. M. Mesías, M. Navarro, N. Martínez-Saez, M. Ullate, M. D. del Castillo, F. J. Morales, Antiglycative and carbonyl trapping properties of the water soluble fraction of coffee silverskin, *Food Res. Int*., 2014, **62**, 1120-1126.
31. A. Farah, M. Monteiro, C. M. Donangelo and S. Lafay, Chlorogenic acids from green coffee extract are highly bioavailable in humans, *J. Nutr*., 2008, **12**, 2309-2315.

32. F. Natella, M. Nardini, F. Belelli, P. Pignatelli, S. Di Santo, A. Ghiselli, F. Violi and C. Scaccini, Effect of coffee drinking on platelets: inhibition of aggregation and phenols incorporation, *Br. J. Nutr.*, 2008, **100**, 1276–1282.
33. F. Natella, M. Nardini, F. Belelli and C. Scaccini, Coffee drinking induces incorporation of phenolic acids into LDL and increases the resistance of LDL to *ex vivo* oxidation in humans, *Am. J. Clin. Nutr*., 2007, **86**, 604-609.

Table 1: MALDI-TOF MS assignments of CGA derivatives.

m/z	Assignment
353.5	$[CGA*+H]^+$ quinone
355.5	$[CGA+H]^+$
375.3	$[CGA+Na]^+$ quinone
377.5	$[CGA+Na]^+$
393.3	$[CGA+K]^+$
399.3	$[CGA+2Na]^+$
415.3	$[CGA+Na+K]^+$
531.4	DHB (matrix) adducts
547.4	DHB (matrix) adducts
551.4	DHB (matrix) adducts
729.6	$[CGA+CGAquinone+Na]^+$
751.6	$[CGA+CGAquinone+2Na]^+$
775.6	$[CGA+CGAquinone+3Na]^+$

*CGA includes the isomers of chlorogenic acid that are undistinguishable by mass spectrometry.

Table 2: Content of total AGEs in samples corresponding to control (BSA), BSA with MGO (BSA+MGO), BSA with MGO and CGA (BSA+MGO+CGA) and BSA with CGA (BSA+CGA) incubated at pH 7.4 and 37 ºC for 72 h. Concentrations assayed were 1mg mL^{-1} BSA, 5 mM MGO and 10 mM CGA. BSA data are considered as initial values.

	Incubation time (h)
	72
BSA	1.01 ± 0.08^{b}
BSA+MGO	1.68 ± 0.13^{a}
BSA+MGO+CGA	0.51 ± 0.08^{c}
BSA+CGA	$0.84 \pm 0.19^{b,c}$

Each value represents the mean (n = 9) ± standard deviation. Different letters denote significant differences ($p < 0.05$) between samples of the same column.

Fig. 1: (a) RP-HPLC chromatograms of CGA (10 mM) incubated at pH 7.4, 37 ºC during 24 h (upper panel) and freshly prepared (lower panel). Peak 1: neochlorogenic acid; Peak 2: cryptochlorogenic acid; Peak 3: chlorogenic acid (b) MALDI-TOF spectra of incubated at pH 7.4, 37 ºC for 24 h (upper panel) and freshly prepared CGA (lower panel).

a

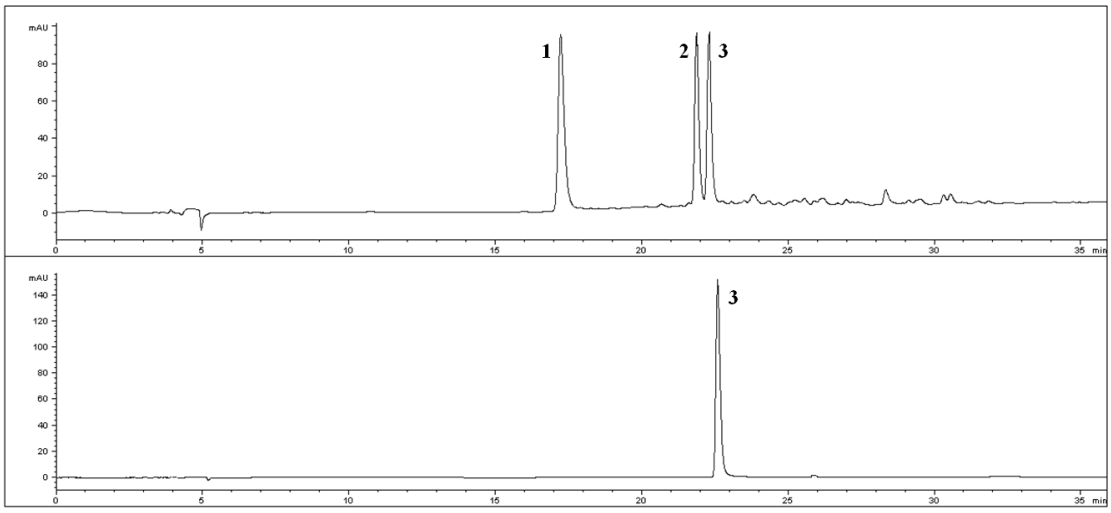

b

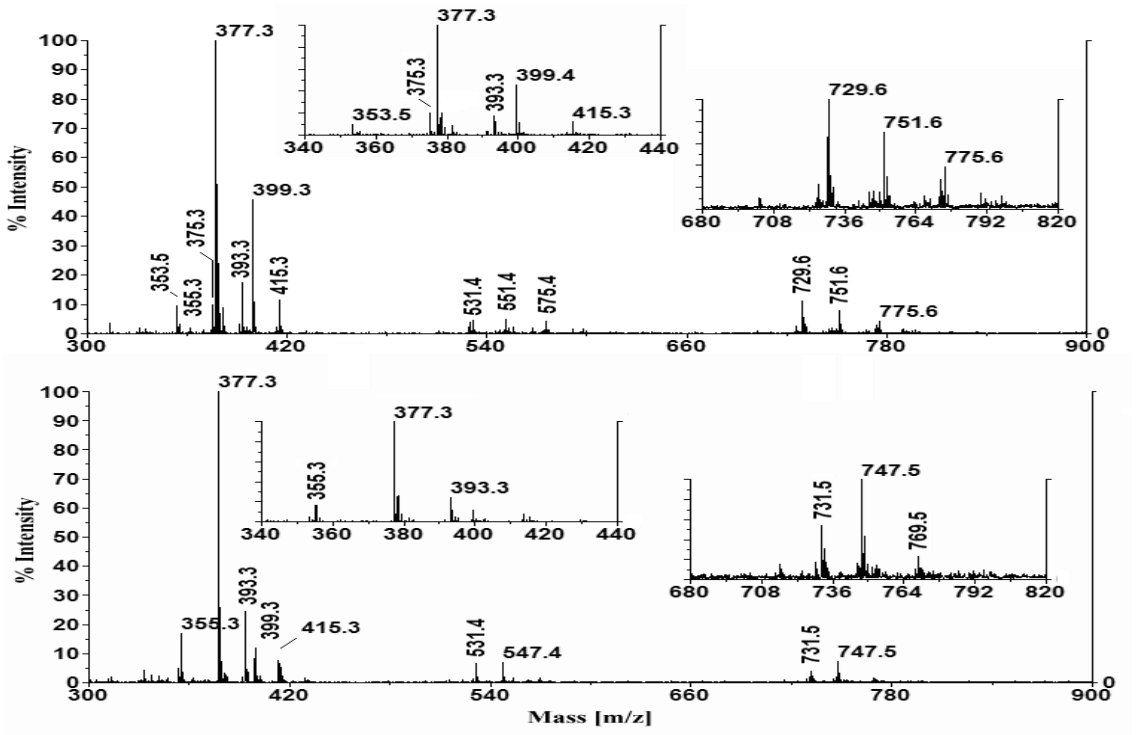

Fig. 2: Changes in the content of free amino groups in samples of control (BSA), BSA with MGO (BSA+MGO), BSA with MGO and CGA (BSA+MGO+CGA) and BSA with CGA (BSA+CGA) incubated at pH 7.4, 37 ˚C at different times during 192 h. Concentrations assayed were 1 mg mL^{-1} BSA, 5 mM MGO and 10 mM CGA. Data are means of triplicate analyses (n=9). Error bars denote the relative standard deviation. Different letters indicate significant differences ($p < 0.001$) within model systems at different times. BSA data are considered as references.

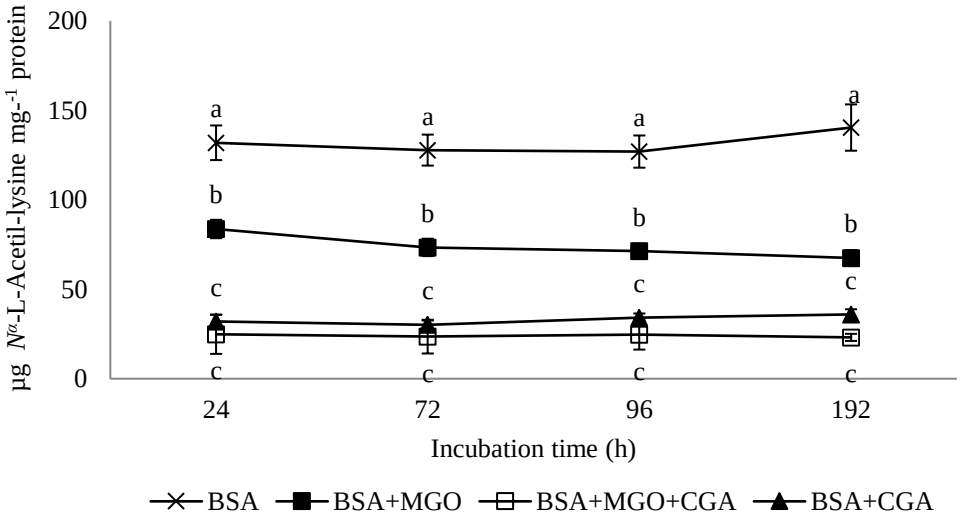

Fig. 3: Time-course of fluorescent AGE formation in samples of control (BSA), BSA with MGO (BSA+MGO), BSA with MGO and CGA (BSA+MGO+CGA) and BSA with CGA (BSA+CGA) incubated at pH 7.4 and 37 ˚C at different times during 192 h. Concentrations assayed were 1 mg mL^{-1} BSA, 5 mM MGO and 10 mM CGA. Data represent relative fluorescence units (RFU) (λ_{exc} 360 nm, λ_{em} 440 nm). Bars represent mean values (n=9) and error bars represent standard deviation. Different letters denote significant differences ($p < 0.05$) within model systems at the different times.

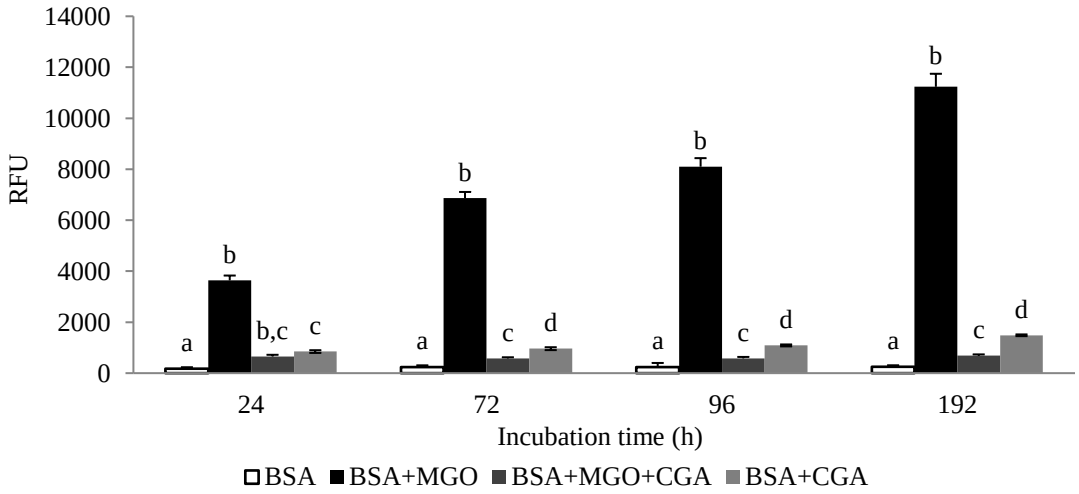

Fig. 4: Time-course of brown compound formation from control (BSA), BSA with MGO (BSA+MGO), BSA with MGO and CGA (BSA+MGO+CGA), BSA with CGA (BSA+CGA) and CGA control (CGA) incubated at pH 7.4, 37 ºC for 192 h. Concentrations assayed were 1 mg mL^{-1} BSA, 5 mM MGO and 10 mM CGA. Data represent relative absorbance at 420 nm at different time points. Bars represent mean values (n=9) and error bars represent standard deviation. Different letters denote significant differences ($p < 0.05$) within model systems at the different times.

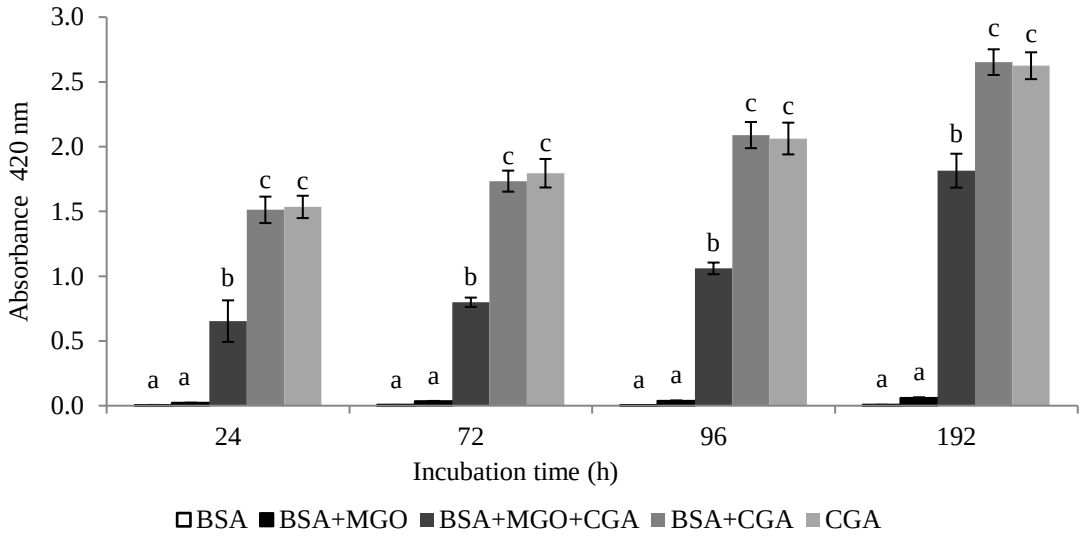

Fig. 5: (a) UV-Vis absorption spectra and (b) content of phenol compounds bound to BSA isolated from samples corresponding to control (BSA), BSA with MGO (BSA+MGO), BSA with MGO and CGA (BSA+MGO+CGA), BSA with CGA (BSA+CGA) and CGA control (CGA) incubated at pH 7.4 and 37 ºC for 72 h**.** Concentrations assayed were 1 mg mL^{-1} BSA, 5 mM MGO and 10 mM CGA. Bars represent mean values (n=9) and error bars represent standard deviation. Different letters denote significant differences ($p < 0.001$) between means.

a

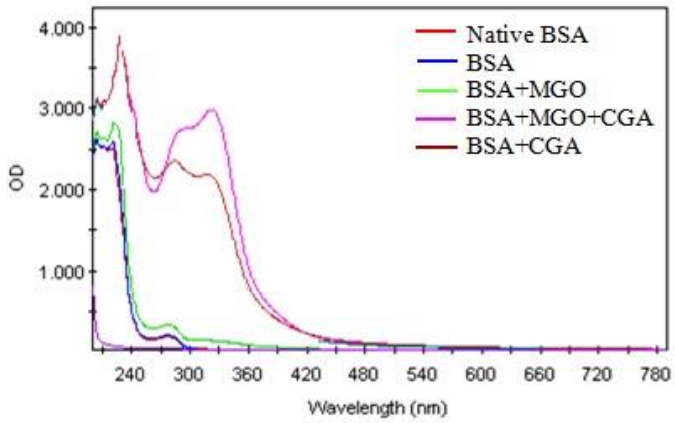

b

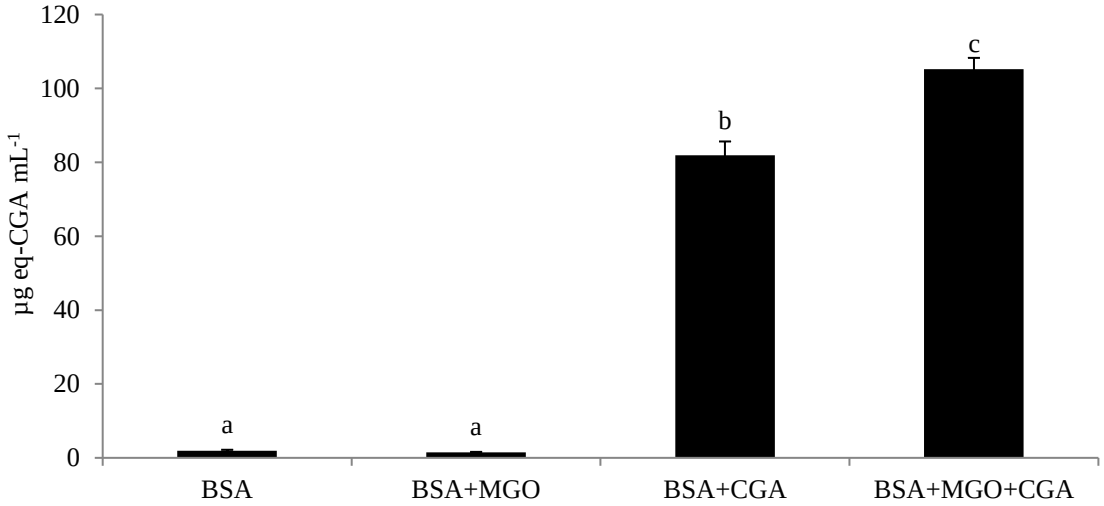

578 **Fig. 6**: MALDI-TOF spectra of BSA control (a), BSA with MGO (b), BSA with CGA (c) and
579 BSA with MGO and (d) incubated at pH 7.4 and 37 ˚C for 72h. Concentrations assayed were 1
580 mg mL^{-1} BSA, 5 mM MGO and 10 mM CGA.

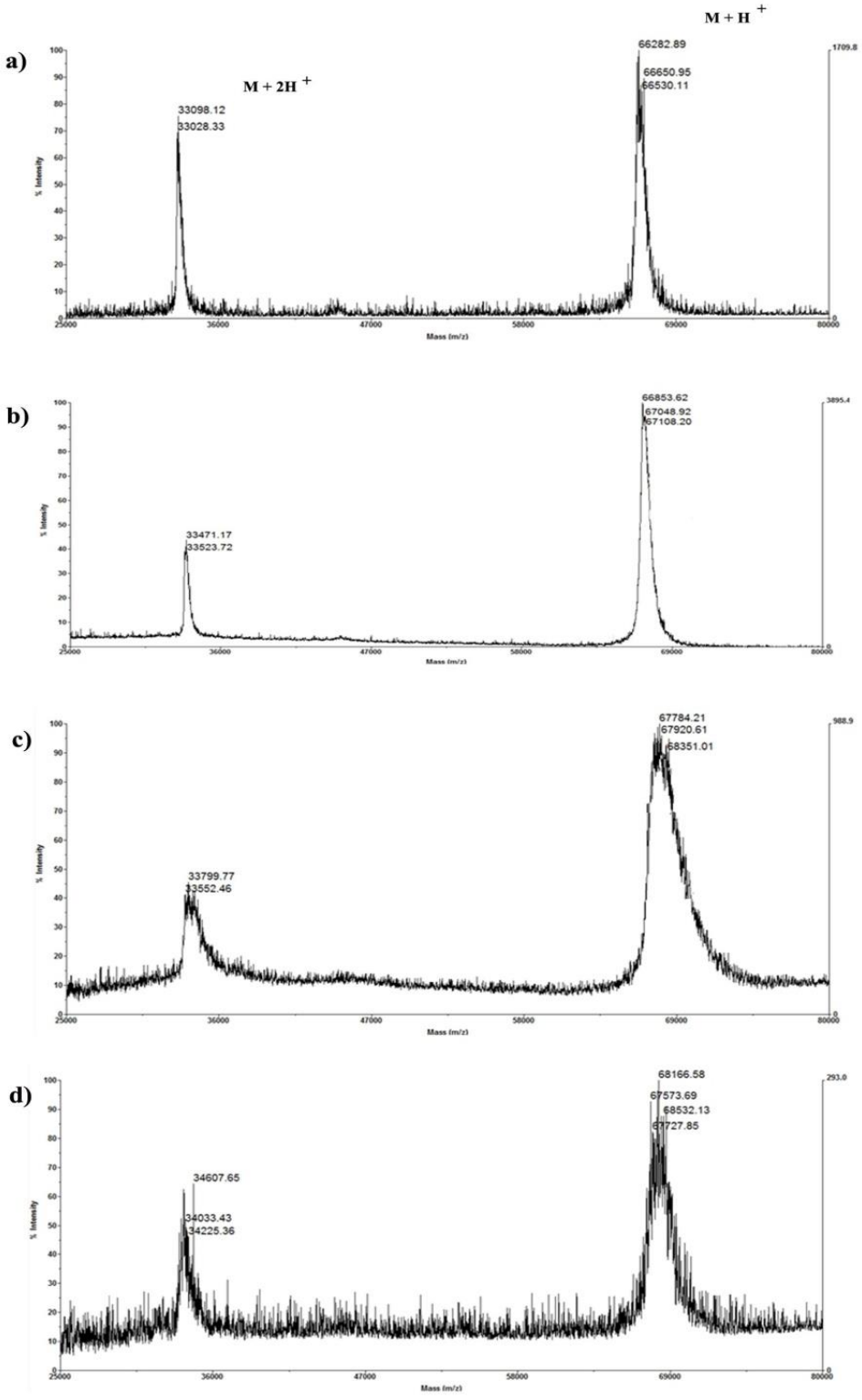

581

582 **Fig. 7**: Antioxidant capacity of the high molecular weight fractions isolated from samples of
583 control (BSA), BSA with MGO (BSA+MGO), BSA with MGO and CGA (BSA+MGO+CGA),
584 BSA with CGA (BSA+CGA) and CGA control (CGA) incubated at at pH 7.4 and 37 ˚C for 72 h.
585 Concentrations assayed were 1 mg mL^{-1} BSA, 5 mM MGO and 10 mM CGA.. Data are expressed
586 as µg eq-CGA mL^{-1}. Bars represent mean values (n=9) and error bars represent standard deviation.
587 Different letters denote significant differences ($p < 0.001$) between means.

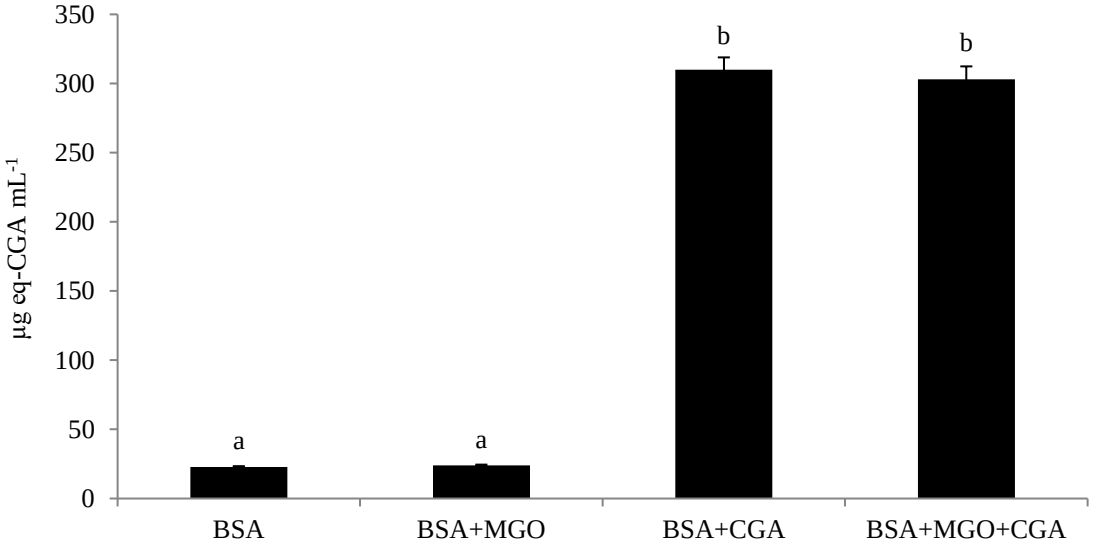

588

589

590

591